of 10 μm. Because of this, a possibility for additional centring of the cold cathode in operating devices has been introduced.

The magnetron anode block is composed of 28 vane-type side resonators. Each of the resonators is 5° wide, and the inner and the outer radii of the resonators are 1.9 and 2.6mm, respectively. The axial length of the anode block is 2mm. The energy is extracted through a slot in one of the resonators, and a waveguide transformer is used in order to match the operating mode with a load. The vacuum seal window at the output waveguide is made of mica which is 0.04mm thick.

The $N/4$–1-mode of the magnetron oscillatory system is used as the working mode. A sufficiently large separation of the eigenfrequencies of neighbouring modes is another important advantage of this mode. Typically, for the oscillatory system described the frequency separation is ~2800MHz with respect to the $N/4$–1-mode, whereas for the π-mode this value is only ~50MHz. Owing to this, additional measures (such as strapping) are not needed in order to guarantee singlemode operation of the SHMs over a relatively large portion of the DC magnetic field strength. This allows the realisation of efficient magnetron operation with a small enough dynamic resistance; typically its value is as low as 200Ω.

If necessary, the resonant frequencies of the 'cold' oscillatory system can be shifted with the end screens of the anode block (see Fig. 2). The possible frequency shift is usually ~500MHz for the working mode.

Table 1: Performance of 95GHz miniature spatial-harmonic magnetron with cold cathode

Output power	1kW
Pulse duration (maximum)	400ns
Duty cycle (maximum)	0.001
Peak anode voltage	6.5kV
Peak anode current	5A
Weight without/with radiators	0.35/0.46kg
Axial length of tube	9cm
Lifetime	2000h

The DC magnetic field strength for the proposed magnetrons is ~0.6T, which is provided by a samarium-cobalt magnet system with a weight of 250g. It should be pointed out that this DC magnetic field value is smaller by a factor of 3 compared with that under magnetron operation utilising the π-mode. The low magnetic field is the main factor for reducing the magnetron size and weight.

Magnetron performance: The performance of the developed and produced low-voltage magnetrons is summarised in Table 1, and a photograph of such a tube is shown in Fig. 3.

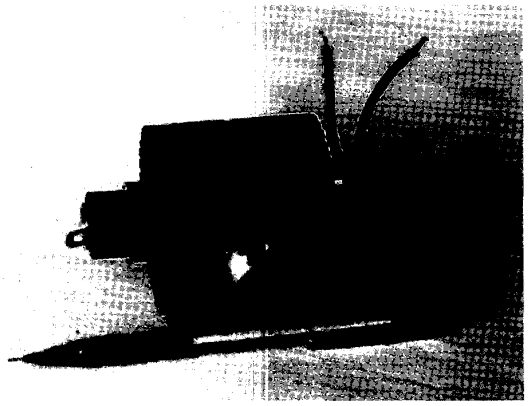

Fig. 3 *Photograph of 95GHz miniature tube*

The variation of the output power over a series of tubes is ~50%, and 1.5kW tubes also occur. The magnetrons do not need special cooling provided that the duty cycle is below 0.0001. At higher values of this parameter (up to 0.001), air cooling is needed, and the magnetrons should contain anode and cathode radiators, which are seen in Fig. 3. A further increase in the average power calls for the application of water cooling.

The minimum build-up time of the magnetron pulse is ~10ns. The measured envelope of the spectrum of a train of pulses practically coincides with that following from the theoretical expression for a train of pulses of rectangular shape and corresponding length. Experiments have shown that the quality of the magnetron pulses is sufficiently high to easily achieve a 0.1m/s Doppler resolution by using conventional modulators and a coherent-on-receiver technique.

Conclusion: The results of this Letter indicate that the principles of spatial-harmonic magnetrons with cold cathodes can be effectively used for the development of low-voltage, miniature tubes. We have presented here a 1kW tube for the 95GHz frequency band. At present, work is in progress on implementing these results in the development of miniature, low-voltage tubes for other frequency bands.

Acknowledgment: This work has been supported by the EC under contract IC15CT980509 and by Deutsche Forschungsgemeimschaft. The authors thank I. Khizshniak, A. Sirov, S. Sosnitsky, A. Suvorov, and V. Volkov for their contributions to the work. D.M. Vavriv is indebted to DAAD for support.

21 September 1999
Electronics Letters Online No: 19991337
DOI: 10.1049/el:19991337

V.D. Naumenko and D.M. Vavriv (*Institute of Radio Astronomy of the National Academy of Sciences of Ukraine, 4, Chervonopraporna St., 310002 Kharkov, Ukraine*)

K. Schünemann (*Technical University Hamburg-Harburg, Arbeitsbereich Hochfrequenztechnik, D-21071 Hamburg, Germany*)

References

1 VIGDORCHIK, I.M., NAUMENKO, V.D., and TIMOFEEV, V.P.: 'Secondary emission cold cathode pulsed magnetrons of the millimeter wavelength band', *Dokl. Akad. Nauk Ukr.*, 1975, **Ser. A**, (7), pp. 633–636

2 NAUMENKO, V., SUVOROV, A., and SIROV, A.: 'Tunable magnetrons of a two-millimeter-wavelength band', *Microw. Opt. Technol. Lett.*, 1996, **12**, (3), pp. 129–131

Power divider with various power dividing ratios

Jong-Sik Lim, Soon-Young Eom and Sangwook Nam

A new power divider which has a completely planar structure and has various output power ratios is presented. This divider does not need any internal isolation resistors, and has almost perfect matching at all ports and perfect isolation characteristics. Such a divider has been fabricated as an example which has output power ratios of 1:1:1, 4:1:1 and 3:2:1 for a three-way divider, and 1:2 and 1:1 ratios for a two-way divider with excellent matching and isolation characteristics.

Introduction: It is well known that any lossless reciprocal three-port network cannot be matched simultaneously. In this Letter, we propose a new six-port network which can be used as a power divider with simultaneous matching and perfect isolation characteristics.

A three-way Wilkinson divider requires a three-dimesional floating common node connecting all isolation resistors together, making fabrication difficult [1]. A two-section hierarchical three-way Wilkinson divider could be used which has a ratio of 1:2 at the first section and equal ratio at the second section, which makes a final ratio of 1:1:1. However, in this case, the characteristic impedance of the transmission line is much higher than 100Ω, hence making it very difficulty to realise [2] on microstrip substrates. An advanced three-way Wilkinson structure which solves the floating node problem was presented in [3]; however it requires additional isolation resistors and wire bonding. Furthermore, the

isolation performances are very sensitive to the length of bonded wire, so its operation frequency is limited to the lower frequency band.

A two-section branch line or ring hybrid with symmetric and asymmetric hierarchy for a three-way power combiner [4] can be realised, but similar problems occur in their realisation. All existing three-way dividers have a fixed division ratio once they have been realised, and cannot be used to realise other dividers with different division ratios.

The power divider presented in this Letter has various output power ratios and a completely planar structure. This divider does not need any internal isolation resistors and additional processes such as wire bonding. This is attractive because it is much easier to realise a three-way divider than any other existing structures. The divider presented in this Letter has excellent matching at all ports and isolation at all isolated ports. Such characteristics are required essentially in all types of power dividers, but to date it has not been easy to obtain them all. A power divider fabricated as an example has 1:1:1, 4:1:1, and 3:2:1 output ratios for a three-way divider, and 1:2 and 1:1 ratios for a two-way divider. The measured results agree well with the predicted performances.

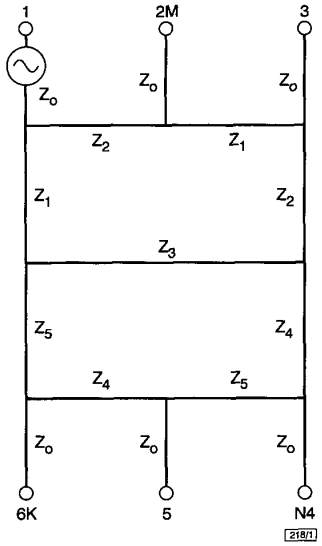

Fig. 1 *Structure of presented power divider*

Structure and analysis of new three-way power divider: Fig. 1 shows the structure of the presented three-way power divider. All transmission lines have the correct characteristic impedance for the realisation. The *S*-parameters of this divider can be expressed as a function of the impedance of the transmission lines as follows:

$$S = [S_{ji}] = f_{ji}(Z_1, Z_2, Z_3, Z_4, Z_5) \tag{1}$$

where $i, j = 1, 2, ..., 6$.

When port 1 is the input port, the incident power is divided into output ports 2, 3, and 6 in the ratio *M*:*N*:*K*, respectively. The electrical length, θ_k (k = 1, 2, 4, 5), of the transmission lines with a characteristic impedance of Z_k is 90°, and θ_3 = 180°. Z_3 is not a critical parameter for the performance of the divider.

For a ratio of *M*:*N*:*K* at the output ports, the characteristic impedance of each transmission line can be expressed by eqns. 2 – 6. This choice gives the output power ratios in Table 1.

$$Z_1 = \sqrt{\frac{\Delta_1}{\Delta_2}} z_o \tag{2}$$

$$Z_2 = \sqrt{\frac{\Delta_1}{M}} z_o \tag{3}$$

$$Z_3 = z_o \tag{4}$$

$$Z_4 = \sqrt{\frac{\Delta_2}{N}} z_o \tag{5}$$

$$Z_5 = \sqrt{\frac{\Delta_2}{K}} z_o \tag{6}$$

where $\Delta_1 = M+N+K$ and $\Delta_2 = N+K$.

When we want to design a 1:1:1 three-way power divider using Table 1, we find that $Z_1 = 1.22Z_o$, $Z_2 = 1.73Z_o$, $Z_4 = 1.41Z_o$, $Z_5 = 1.41Z_o$ and $Z_3 = Z_o = 50\Omega$. This divider works as a different divider with a 3:2:1 division ratio when the input port is port 4 or 6, and a 4:1:1 ratio with port 3 as the input.

Table 1: Output power dividing ratios for each input port

j \ i	1	2	3	4	5	6
1	0	$\frac{M}{\Delta_1}$	0	$\frac{N}{\Delta_1}$	0	$\frac{K}{\Delta_1}$
2	$\frac{M}{\Delta_1}$	0	$\frac{\Delta_2}{\Delta_1}$	0	0	0
3	0	$\frac{\Delta_2}{\Delta_1}$	0	$\frac{MN}{\Delta_1\Delta_2}$	0	$\frac{MK}{\Delta_1\Delta_2}$
4	$\frac{N}{\Delta_1}$	0	$\frac{MN}{\Delta_1\Delta_2}$	0	$\frac{K}{\Delta_2}$	0
5	0	0	0	$\frac{K}{\Delta_2}$	0	$\frac{N}{\Delta_2}$
6	$\frac{K}{\Delta_1}$	0	$\frac{MK}{\Delta_1\Delta_2}$	0	$\frac{N}{\Delta_2}$	0

Table 1 also shows the performances of the proposed structure used as a two-way power divider. When port 2 is the input port, the power is divided into ports 1 and 3 with a 1:2 ratio. The other ports are all isolated. The same situation occurs when the incident power at port 5 is equally divided into ports 4 and 6.

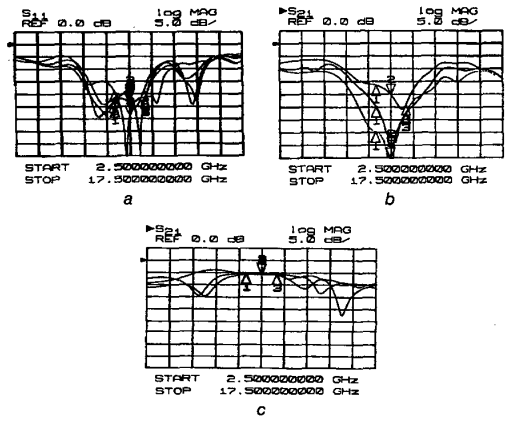

Fig. 2 *Measured performance as 1:1:1 power divider*

a Matching
b Isolation
c 1:1:1 power ratio

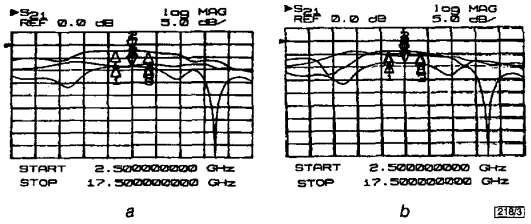

Fig. 3 *Measured other power ratios of three-way power divider*

a 4:1:1 dividing
b 3:2:1 dividing

Measured performances: A three-way power divider has been realised using eqns. 2 – 6 and its performance measured. The measured performances of the three-way divider are shown in Figs. 2 and 3. First, Fig. 2 shows the performances of the 1:1:1 three-way divider when port 1 is the input port. We can see that this power

divider has excellent matching and isolation characteristics. Fig. 3 shows results for the 4:1:1 and 3:2:1 dividing ratios in the three-way divider. Finally, Fig. 4 shows the performances for 1:2 and 1:1 two-way dividers with excellent isolation.

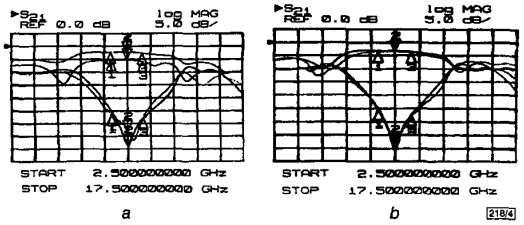

Fig. 4 *Measured performances as two-way power divider*

a 1:2 division
b 1:1 division

Conclusion: A new power divider which does not need any internal isolation resistors, which are required for the Wilkinson structure, and which has a totally planar structure has been designed and realised. The divider can be used as three types of three-way (1:1:1, 4:1:1 and 3:2:1) and two different two-way (1:2 and 1:1) divider. Because this divider has various output power ratios depending on the input port, it is very adaptable for practical applications. Another feature of this divider is the ability to extend it to an N-way power divider and the possibility of obtaining arbitrary power ratios using simple equations (eqn. 2 – 6).

8 September 1999
Electronics Letters Online No: 19991315
DOI: 10.1049/el:19991315

Jong-Sik Lim and Sangwook Nam (*School of Electrical Engineering, Seoul National University, San-56-1, Shilim-Dong, Kwanak-Gu, Seoul, 151-742, Republic of Korea*)

Soon-Young Eom (*Electronics and Telecommunications Research Institute, YuSong PO Box 106, Taejon, 305-600, Republic of Korea*)

References

1 WILKINSON, E.J.: 'An N-way hybrid divider', *IRE Trans.*, 1960, **MTT-8**, pp. 116–118
2 POZAR, D.M.: 'Microwave Engineering' (John Wiley & Sons, Inc., New York, 1998), 2nd edn., pp. 363–368
3 MAURIN, D., and WU, K.: 'A compact 1.7–2.1GHz three-way power combiner using microstrip technology with better than 93.8% combining efficiency', *IEEE Microw. Guid. Wave Lett.*, 1996, **6**, (2), pp. 106–108
4 REED, J., and WHEELER, G.J.: 'A method of analysis of symmetrical four-port networks', *IRE Trans.*, 1956, **MTT-4**, pp. 246–252

'Mechanical' neural learning for blind source separation

S. Fiori

A class of learning models derived from the study of the dynamics of an abstract rigid mechanical system is presented. Application to blind source separation is illustrated through computer simulations.

Introduction: The learning of a connection (weight) matrix by a neural network may be conceived as an optimisation problem, which in some cases may be constrained by the nature of the task that the network should perform. In neural blind source separation [1–4, 8, 9] by pre-whitening (see [4, 9] and references therein), the separation network that works on pre-whitened data has to learn an orthonormal connection matrix, which is a $p \times m$ ($m \leq p$) matrix $\mathbf{W}$ such that $\mathbf{W}^T\mathbf{W} = \mathbf{I}_m$. When a standard gradient steepest ascent/descent method is used for updating the weight matrix, it is necessary to include into the optimisation system some mechanism that keeps $\mathbf{W}$ orthonormal; common approaches are based on the projection of the updated matrix onto the orthonormal group by Gram-Schmidt orthogonalisation or singular value decomposition, and the Lagrange multiplier method based on a penalty term such as, for instance, the measure $\|\mathbf{W}^T\mathbf{W} - \mathbf{I}_m\|_F$; however, imposing the mentioned constraint can be quite problematic in practice [5].

In [6, 7], we proposed a learning rule for orthonormal learning derived by a study of the dynamics of an abstract rigid system of masses, by showing that the relationships which describe the dynamics of such a system may be readily interpreted as adapting equations. The aim of this Letter is to apply the learning theory for solving blind source separation problems.

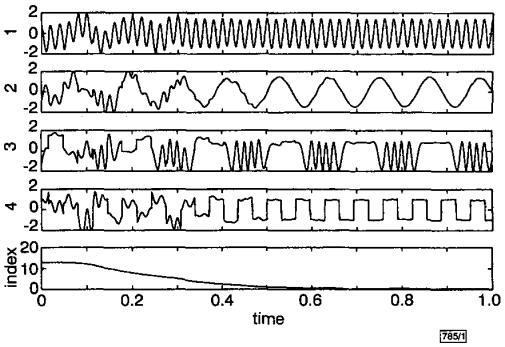

Fig. 1 *Four source signal separation*
Outputs of network and separation index against time

Learning algorithm derivation: Let $S = \{[2m_i, \mathbf{w}_i]\}$ be an abstract rigid system of masses, where the m vectors $\mathbf{w}_i \in \mathbb{R}^p$ ($p \leq m$) represent the instantaneous positions of the m masses m_i, in a co-ordinate system originating in O. Such masses are positioned at constant (unitary) distances from O along mutually orthogonal axes.

Masses m_i move in the space $\mathbb{R}^p$ where a physical point with negligible mass also moves; its position with respect to O is described by a vector $\mathbf{x}$. The point exerts a force on each mass and the set of forces so generated causes S to move. Furthermore, masses move in a homogeneous and hysotropic fluid endowed with a non-negligible viscosity the resistance of which brakes the system motion. The dynamics of this system is described by theorem 1.

(i) *Theorem 1 [6]:* Let S be the physical system described above: denote by $\mathbf{F}$ the matrix of the active forces, $\mathbf{P}$ the matrix of the viscosity resistance, $\mathbf{H}$ the angular speed matrix, $\mathbf{M}$ the diagonal matrix of the masses and $\mathbf{W}$ the matrix of the instantaneous positions of the masses. In the special case where $\mathbf{M} = \mathbf{I}$, the motion of the system can be represented by the following equations:

$$\frac{d\mathbf{W}}{dt} = \mathbf{H}\mathbf{W} \qquad \mathbf{P} = -\mu\mathbf{H}\mathbf{W} \tag{1}$$

$$\frac{d\mathbf{H}}{dt} = \frac{1}{4}[(\mathbf{F}+\mathbf{P})\mathbf{W}^T - \mathbf{W}(\mathbf{F}+\mathbf{P})^T] \tag{2}$$

with μ a positive parameter termed the viscosity coefficient.

The above result states that if $\mathbf{W}(0)$ is orthonormal, then for $t > 0$ $\mathbf{W}(t)$ remains orthonormal, i.e. $\mathbf{W}^T(t)\mathbf{W}(t) = \mathbf{I}_m$. This is due to the rigidity of the system which can only rotate around O.

Eqns. 1 and 2 may be assumed to form an adapting rule for neural layers with weight matrix $\mathbf{W}$. The proposed learning algorithm applies indistinctly to any neural layer described by $\mathbf{y} = \mathbf{A}[\mathbf{W}^T\mathbf{x} + \mathbf{w}_0]$, where $\mathbf{x} \in \mathbb{R}^p$, $\mathbf{W}$ is $p \times m$, with $m \leq p$, $\mathbf{w}_0$ is a generic biasing vector in $\mathbb{R}^m$ and $\mathbf{A}[\cdot]$ is an $m \times m$ diagonal activation operator. The learning rule (eqns. 1 and 2) can be used to solve orthonormal problems.

To illustrate how the above dynamical system can be used for optimisation, we suppose that the force terms derive from a potential energy function (PEF) U; therefore we assume [6] that

$$\mathbf{F} \stackrel{\text{def}}{=} -2\frac{\partial U}{\partial \mathbf{W}} \tag{3}$$

Generally speaking, we can assume that U is dependent on $\mathbf{W}$ only, in the sense that $U = E_{\mathbf{x}}[u(\mathbf{W}, \mathbf{x}, \mathbf{y})]$. Recalling that a (dissi-